공학석사학위논문

등유공급이 질화 알루미늄 마이크로 방전 가공 성능에 미치는 영향

Effect of Kerosene Supply on the Performance of Micro-Electrical Discharge Machining of Aluminum Nitride

2020 년 2 월

서울대학교 대학원

기계항공공학부

김 대 녕

등유공급이 질화 알루미늄 마이크로 방전 가공 성능에 미치는 영향

Effect of Kerosene Supply on the Performance of Micro-Electrical Discharge Machining of Aluminum Nitride

지도교수 안 성 훈

이 논문을 공학석사 학위논문으로 제출함

2019 년 10 월

서울대학교 대학원

기계항공공학부

김 대 녕

김 대 녕의 공학석사 학위논문을 인준함

2019 년 12 월

위 원 장 김 종 원

부위원장 안 성 훈

위 원 이 윤 석

Abstract

Dae Nyoung Kim

School of Mechanical and Aerospace Engineering

The Graduated School

Seoul National University

As interest in aluminum nitride (AlN), one of the high-performance ceramics, has been rapidly increasing, many researchers have put a lot of efforts to machining it. Since AlN is classified as a difficult-to-cut material, the EDM process using an assisting electrode is emerging as an effective machining method. Kerosene, as a dielectric fluid, plays the important role in the formation of a conductive carbon layer called as the assisting electrode, which deposited on the surface of the workpiece and inducing discharge. Most of the previous methods used the hollow electrodes to stably feed the dielectric fluids through their center hole. However, in the case of micro-EDM, their extremely small electrode diameter makes it difficult to fabricate a through hole in the electrode and very narrow gap hinders the flow of dielectric fluid. In order to overcome feeding problems in micro-EDM of AlN, in this study, two kinds of kerosene feed enhancing methods are introduced: one is to use a D-shape electrode to obtain a wider asymmetric flow channel; and the other is to use graphite powder mixed kerosene (GPMK) and increase the gap between the tool and

the workpiece. Flow simulation results show that both methods have the effect of discharge gap widening that promotes kerosene flow, and the experimental results show similar results as well. When using a D-shape electrode, the material removal rate (MRR) increased under the negative electrode condition but fast tool wear was observed. On the other hand, with GPMK, the MRR increased 64% and the electrode wear decreased 73% compared to the conventional ways under the positive electrode condition.

Keywords: Aluminum nitride; micro-EDM; Assisting electrode method; Graphite-powder-mixed-kerosene

Student number: 2018-20023

Contents

List of Figures

List of Tables

List of Symbols

C_1	= Capacitance 1, [nF]
I_{AE}	= Current on system, [A]
I_{CL}	= Current on CL, [A]
I_L	= Current on stray inductance, [A]
L	= Stray inductance, [H]
R_1	= Resistance 1, [Ω]
$R_{sys,CL}$	= Resistance of system, CL, [Ω]
t	= Time, [ns]
V	= Open voltage, [V]

Chapter 1

Introduction

Because aluminum nitride (AlN) exhibits superior properties, such as high hardness, thermal conductivity, and chemical resistance, it is classified as a hard-to-cut material. AlN, a vital substrate material, is used for microelectronics, semiconductor packaging, and micro-electromechanical systems. It has high thermal conductivity and a low thermal expansion coefficient, being an electrical insulator with high wear and thermal and chemical resistance properties [1-3]. Micro-machining of AlN is required for these types of uses; however, due to the outstanding properties of AlN, the machining of micro-scale features using traditional cutting methods is difficult because of the risk of tool wear and breakage due to excessive tool loads during the process. In addition, traditional cutting techniques used for sintered AlN require expensive tools, such as polycrystalline diamond [4, 5].

Many attempts have been made to micromachine AlN, with some researchers using un-sintered or pre-sintered ceramic machining [6, 7]. However, these methods require a sintering process, whereby shrinkage occurs and compensation is required. Moreover, the un-sintered ceramic machining method can result in edge cracks because of the low brittleness of green body AlN. Gilbert et al. [8] investigated the laser-assisted machining of AlN using UV and a near-infrared Nd:YAG laser. However, the laser machining process is not suitable for AlN because this method has low levels of accuracy, such as tapered shape channels and low surface roughness.

Lumpp et al. [9] fabricated thru-holes in AlN using an excimer laser, but a highly tapered crater was prematurely generated at the end of the holes due to the propagation of shock waves through the substrate. Katahira et al. [10] produced an extremely flat surface roughness of 0.008 μm Ra using electrolytic in-process dressing (ELID) for the grinding of AlN; however, ELID grinding has a low material removal rate (MRR) and produces limited shapes.

For the micromachining of AlN, electrical discharge machining (EDM) has been found to be relatively fast and highly accurate [11]. EDM is widely used for the machining of hard-to-cut and brittle materials due to the thermal ablation of the discharge, which occurs in the dielectric fluid. Furthermore, as this type of machining is a non-contact process, there is no tool breakage, even during micromachining. In addition, because EDM can only be used for electrically conductive workpieces, it can be indirectly applied to AlN micromachining because AlN is a non-conductive ceramic. Hence, Mohri et al. [12] proposed an assisting electrode (AE) for the EDM of non-conductive ceramics.

During AE EDM, the ready supply of kerosene to the machined surface is crucial. Carbon decomposed from the kerosene deposited on the non-conductive ceramic surface acts as a conductive layer (CL) for a stable discharge. However, during micro EDM, it is difficult to maintain sufficient kerosene on the machined surface due to a narrow discharge gap: the gap between the electrode and the workpiece is smaller than 10 μm. As micro-holes are deepened during micro ED-drilling, the use of a cylinder tool electrode makes it more difficult to supply kerosene to the machined surface to stably generate a CL. To solve this problem, a tubular electrode can be

used to directly supply kerosene to the machined surface through an inner hole [13]. However, as the tool size decreases, it becomes more difficult to use a tubular electrode. Positive tool polarity can increase machinability by adding aluminum decomposed from the AlN for the generation of a CL [14]; however, tool wear is increased due to high energy distribution at the anode [15].

To solve these two problems, while maintaining the negative polarity of a tool electrode, this study proposed using a D-shape tool electrode and graphite-powder-mixed kerosene (GPMK). A D-shape tool electrode enlarges the kerosene flow path by changing the geometrical form of the tool electrode. Owing to the bridge effect, GPMK is used as a dielectric fluid in AE EDM to broaden the discharge gap between a tool electrode and a workpiece [16]. To verify the effects of these methods, flow simulations of both cases were performed. A parameter test was also performed to determine the optimal machining conditions for open voltage and capacitance. A performance evaluation of these two methods was then conducted to compare them with the conventional micro-EDM of AlN, which uses positive tool polarity.

In the following sections, the kerosene supply mechanism is explained in more detail. Several simulation and experimental results are then presented to support our explanation, and the machining conditions for the micro ED-drilling of AlN are also optimized. The paper concludes with a discussion of kerosene supply methods considering the experimental and simulated results presented herein.

Chapter 2

Experimental setup

Figure 2.1 shows the schematic of an experimental setup consisting of a precision three-axis stage (806CT for X-Y, 404XR for Z, Parker, USA), a feed controller (Clipper, Delta Tau, USA), a RC discharge circuit module and an dielectric fluid feed and circulation system. The feed of the electrode is controlled to keep the voltage across the resistor (R_2) constant (CV mode). The mechanical stirrer was used to maintain the graphite concentration in dielectric fluid, Kerosene. A copper (an initial assisting electrode) plated 0.3 mm thick AlN substrate was used for the workpiece. Table 2.1 summarizes the properties of AlN. A cylindrical tungsten carbide rod with a diameter of 100 μm was used as an electrode fabricated by wire electric discharge grinding [17]. Figure 2.2 shows the two types of micro electrodes used in micro EDM. Table 2.2 summarizes the machining conditions.

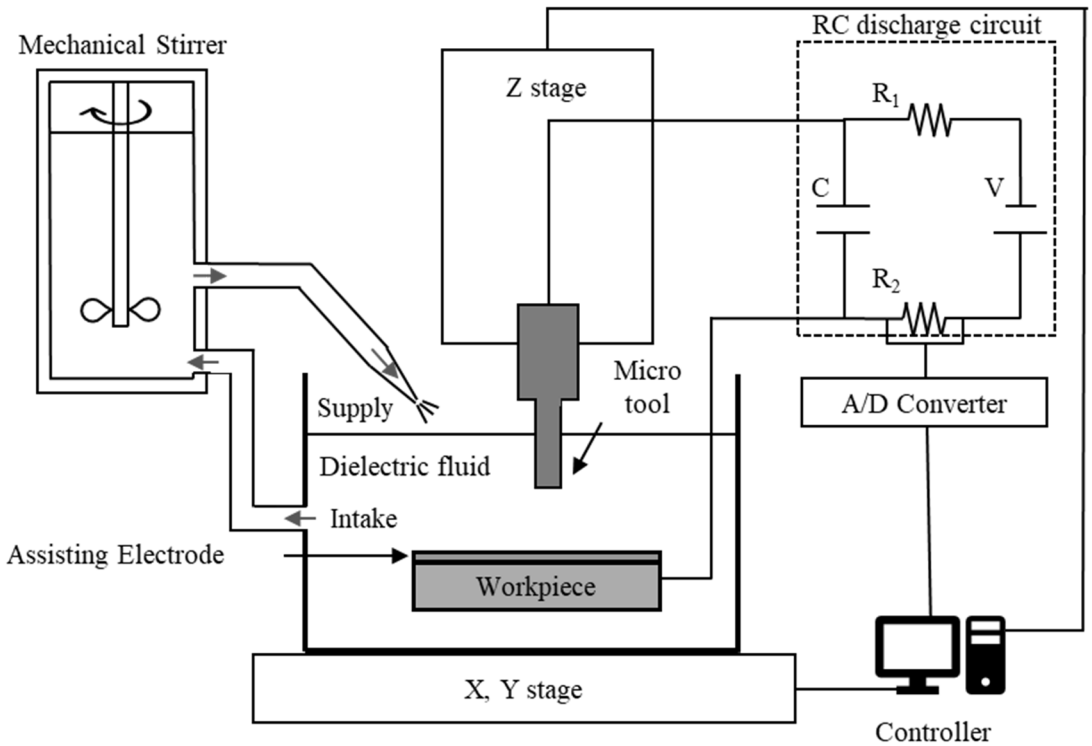

Figure 2.1 Schematic experimental setup

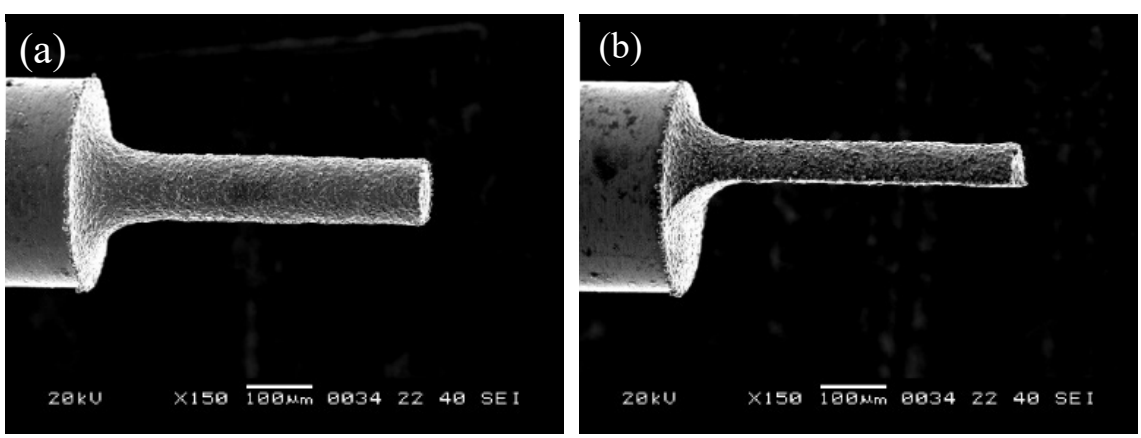

Figure 2.2 (a) Cylinder and (b) D-shape tool types

Table 2.1 AlN properties

	AlN
Melting point [K]	2470
Sublimation point [K]	2790
Density [g/cm^3]	3.3
Thermal conductivity [W/m·K]	174
Volume resistivity [Ω·cm]	>10^{14}
Bending strength [Mpa]	450
Hardness [HV]	1100

Table 2.2 Machining conditions

Machining type	Drilling		
Workpiece	AlN (thickness: 300 μm)		
Assisting electrode	Copper (thickness: 20 μm)		
Tool material	WC-Co		
Tool type	Cylinder		D-shape
Dielectric fluid	Pure kerosene (PK)	Graphite-powder-mixed kerosene (GPMK), particle size: 40 nm, concentration: 2 g/L)	Pure kerosene (PK)
Open voltage [V]	100, 125, 150		
Capacitance [nF]	10, 15, 20		

Chapter 3

Results and discussion

3.1 CL generation for AE EDM

In AE EDM, the most important factor is the continuous generation of a CL. In previous research of AE EDM, carbon decomposed from kerosene adhered to the machined surface served as a CL [18]; therefore, the supply of kerosene is vital for generating a CL. Table 3.1 shows the results of the energy dispersive spectrometry analysis undertaken during AE ED drilling performed on AlN under conditions of V = 125 V and C_1 = 10 nF; as shown, the atomic percentage of carbon in the CL increased by up to 34.54%. This result verified that the CL is composed of carbon during AlN EDM; hence, it is necessary readily supply kerosene as a source of carbon for CL generation.

Table 3.1 Energy dispersive spectrometry results for micro ED-drilling of AlN with kerosene (non-machined AlN)

Element	**Atomic % (Reference)**
Carbon	34.54 (9.44)
Nitrogen	23.35 (39.36)
Oxygen	8.67 (9.05)
Aluminum	32.79 (42.16)
Cobalt	0.11
Tungsten	0.54
Totals	100.00

3.2 CL generation monitoring

This research monitored the status of CL generation using the peak current of the discharge waveform. The value of the peak current is directly related to the resistance of the CL. Figure 3.1 is the equivalent circuit of the RC discharge generator used in this study as the discharge occurred [19]. R_{sys} indicates the system resistance, which stems from the physical components of the system, such as the electrical wires and a mandrel. According to the modeling, the waveform of the discharge can be predicted by the following equation:

$$\frac{\mathrm{d}^2 I_L(t)}{dt^2} + \left(\frac{1}{R_1 C_1} + \frac{R_{sys}+R_{CL}}{L}\right)\frac{dI_L(t)}{dt} + \frac{R_1+R_{sys}+R_{CL}}{R_1 L C_1} I_L(t) = \frac{V}{R_1 L C_1} \qquad (1)$$

The resistance of the CL can then be calculated using Eq. (2). I_{AE} and I_{CL} are currents measured with an oscilloscope when the tool contacts the AE and CL, respectively. The resistance of the CL can be calculated using the difference between the AE and CL contact cases.

$$\mathrm{R_{CL}} = \frac{V}{I_{\mathrm{CL}}} - \frac{V}{I_{\mathrm{AE}}} \qquad (2)$$

Figure 3.2(a) shows the simulated result using the calculated R_{CL}. Figure 3.2(b) shows the discharge current waveform observed using an oscilloscope during the actual machining. The machining was performed under conditions of V = 125 V and C_1 = 10 nF. As shown in Figures 3.2(a) and (b), the peak currents were 0.54 A and 0.53 A, respectively, and these two current waveforms were almost identical. This means that the current value was closely connected with R_{CL}, and the status of the

CL generation could be monitored by the value of the peak current.

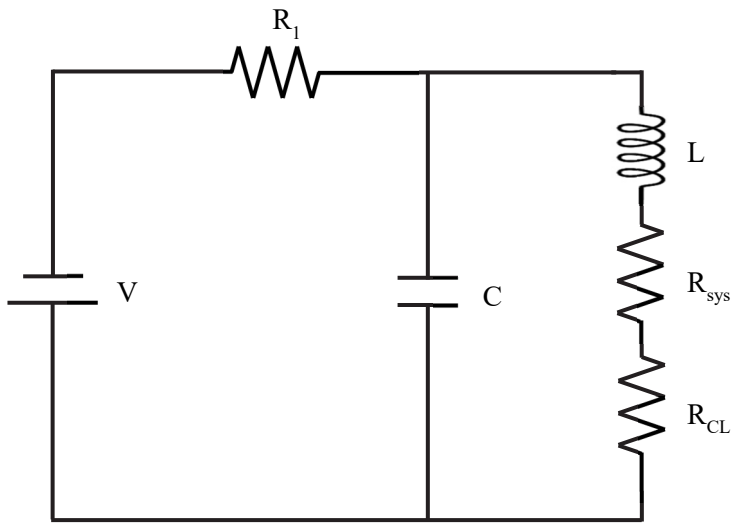

Figure 3.1 RC discharge generator equivalent circuit

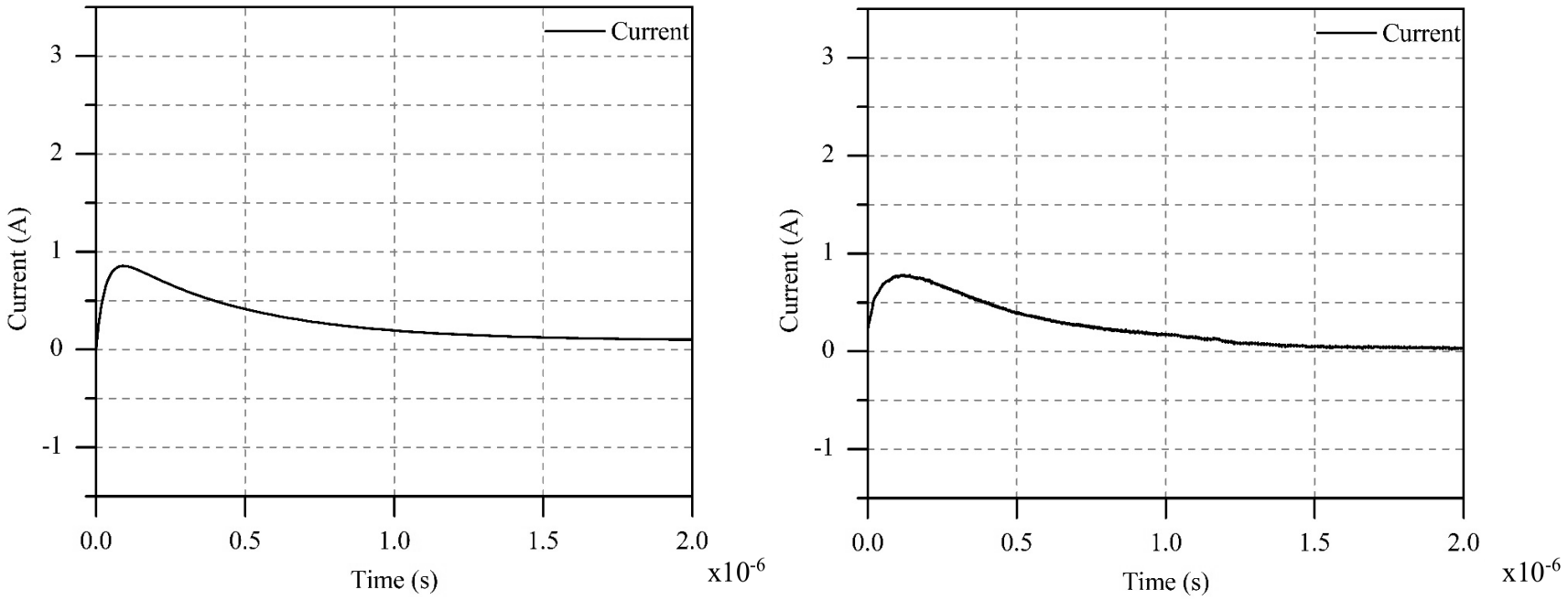

Figure 3.2 (a) Simulated discharge current wave at calculated R_{CL} and (b) oscilloscope measured discharge current wave

3.3 Effects of kerosene supply

The supply of pure kerosene (PK) is an important factor for the stable generation of a CL. Figure 3.3 shows the discharge gap according to the dielectric fluid and open voltage. In the case of PK, the discharge gaps of all the three open voltages were narrower than those for GPMK. During micro ED-drilling, these narrow discharge gaps can hinder the supply of PK to the machined surface; however, the use of GPMK solves this issue. In addition, a D-shape tool enhances the supply of PK by changing the shape of the tool electrode and securing the PK flow path.

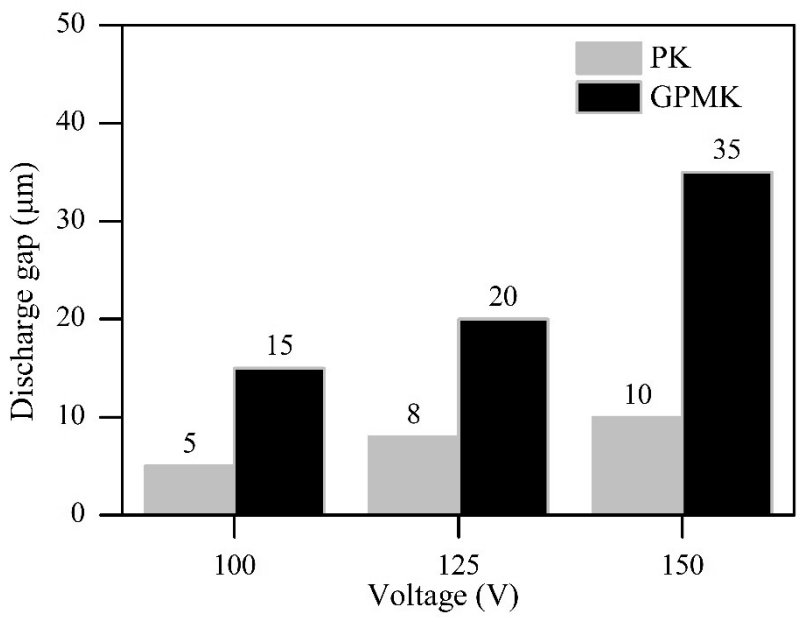

Figure 3.3 Pure kersosene (PK) and graphite-powder-mixed kerosene (GPMK) discharge gaps

3.3.1 Flow simulation

To determine the effects of an enlarged kerosene flow path using a D-shape tool electrode and GPMK, computational fluid dynamics (CFD) software was used to simulate the flow of kerosene onto a machined surface. The simulation was conducted using SOLIDWORKS Flow Simulation software (ver.2017). The diameter of the drilled holes was 120 μm, and the depths were 50, 100, and 150 μm, respectively, for the three cases. The dynamic viscosities of the dielectric fluids were 1.67 cP for the PK and 1.66 cP for the GPMK. The tool diameter for both the cylinder tool with PK and the D-shape tool with PK was 100 μm; however, for the cylinder tool with GPMK, the diameter was 50 μm because the discharge gap at 150 V was 10 μm for the PK and 35 μm for the GPMK. The rotating speed of the tool was 500 rpm, and the flow rate for both the PK and GPMK was set at 2 ml/s, which was similar to the experimental conditions. The simulation results are illustrated in Figure 3.4.

For the cylinder tool with PK, the flow of kerosene onto the machined surface started to stagnant at a drilled depth of 100 μm. This indicted that the discharge gap was narrow and the kerosene could not flow readily. In contrast, for the D-shape tool with PK, the kerosene continued to readily flow onto the machined surface at greater drilled depths than for the cylinder tool with PK. Likewise, for the cylinder tool with GPMK, the kerosene flow onto the machined surface was maintained. Therefore, both the D-shape tool and the GPMK facilitated the supply of kerosene onto the machined surface and the generation of a CL, for stable discharge.

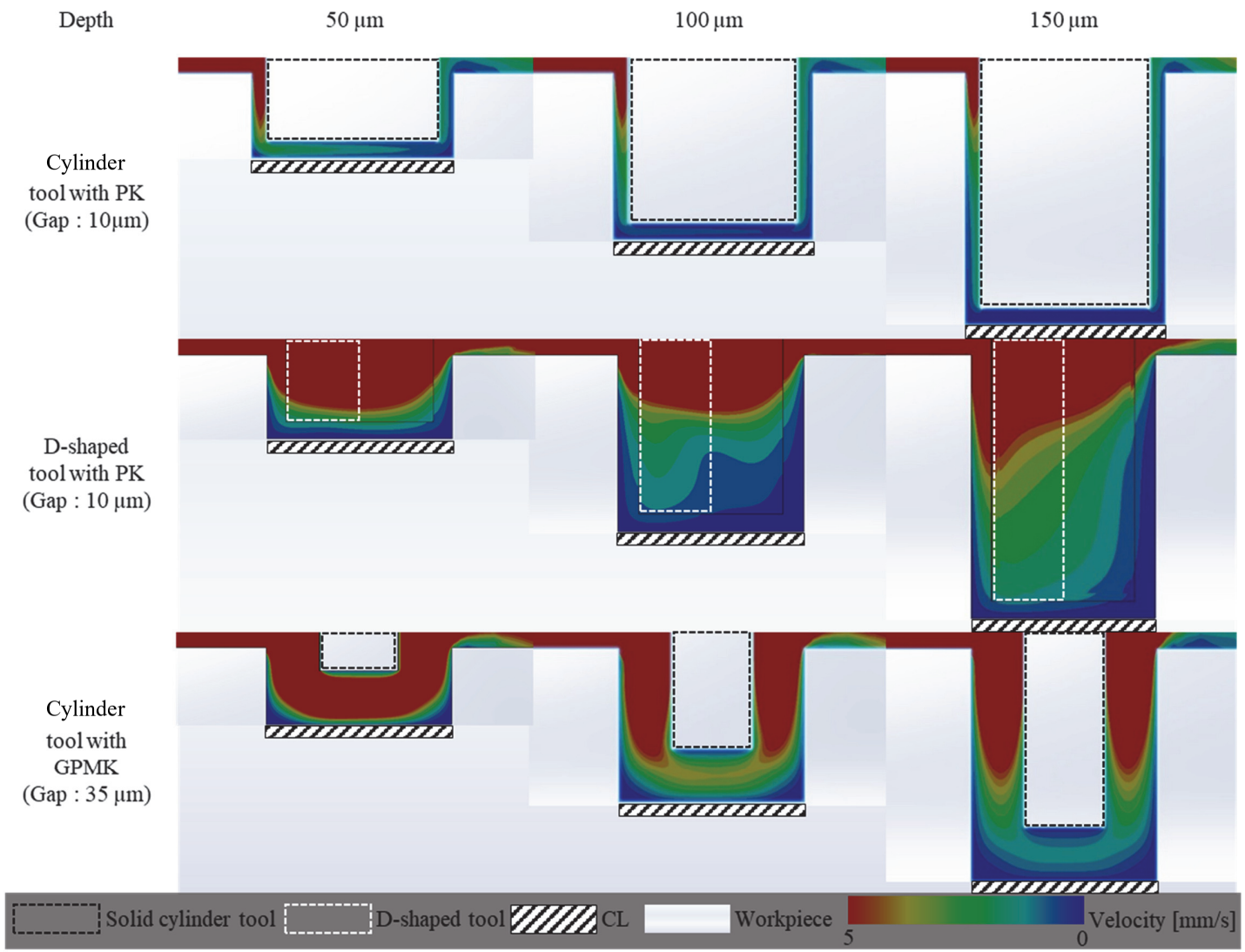

Figure 3.4 Simulation results

3.3.2 Peak current with tool position

The peak value of the discharge current was measured according to the tool position. All the tool electrodes were negatively charged. The results are illustrated in Figure 3.5. In the case of the cylinder tool with PK, at greater drilling depths, the peak current decreased and the machining could not proceed beyond a depth of 175 um. This indicated that the resistance of the CL continuously increased with tool depth, and the PK supply was insufficient due to the narrow discharge gap; therefore, insufficient CL was generated for the machining. However, in the case of the D-shape tool with PK, even though the peak current also decreased, almost all the values were higher than those for the cylinder tool with PK, and the tool finally reached the target position. This indicated that a D-shape tool can more readily supply kerosene to a machined surface because of its asymmetrical form than a cylinder tool. In contrast, for the cylinder tool with GPMK, the peak current remained at a similar value although the tool position changed. This indicated that the generation of the CL was stable from the beginning to the end of the machining, and a thin CL was generated by the reduced explosion pressure of the dielectric fluid due to the broadening discharge gap. Hence, the resistance of the CL was higher than that of the other two cases. Even though the peak current of the cylinder tool with GPMK was lower than that for the other two cases, drilling to a depth of 300 μm was possible because of the machining characteristics of the GPMK, which increased the discharge frequency and the MRR by shortening the ignition delay time [19]. Therefore, the total discharge energy of the GPMK was much higher than for the PK; thus, machining was possible even though the peak current of the GPMK was lower than for the PK.

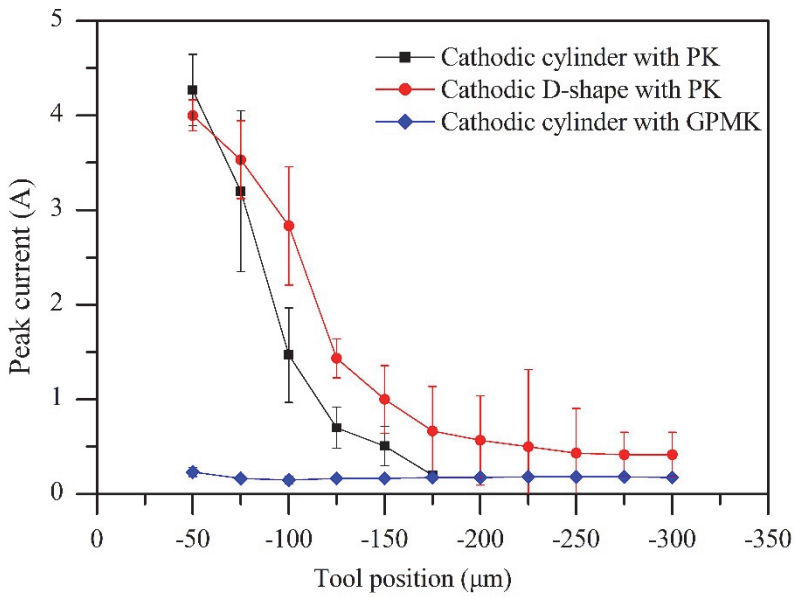

Figure 3.5 Peak current changes with tool position

3.4 Parameter test for optimal conditions

In this section, the MRRs and RWRs of the three machining methods are compared. Kaneko et al. [14] used an anodic cylinder tool electrode with PK for effective AlN machining. Therefore, the results of machining with a cathodic D-shape tool electrode with PK and a cathodic cylinder tool electrode with GPMK were compared with those of an anodic cylinder tool electrode with PK. Hereafter, these methods are called cathodic D-shape with PK, cathodic cylinder with GPMK, and anodic cylinder with PK, respectively. MRR was calculated by dividing the machined depth by the machining time, while RWR was calculated by dividing the wear length by the machined depth. The MRR and RWR were evaluated with respect to several values of open voltage (100, 125, and 150 Vs) and capacitance (10, 15, and 20 nFs). The tool diameter was 100 μm for all the parameter tests, and for each machining condition, the tool was commanded to reach a depth of 300 μm. The results are illustrated in Figure 3.6.

Machining was impossible using a cathodic D-shape with PK with an open voltage of 150 V because the excessive explosion pressure of the dielectric fluid caused a disconnection between the AE and the CL on the machined surface. In terms of the open voltage, 100 V was better than 125 V. Between the three capacitance values, 15 nF showed the optimal results for the cathodic D-shape with PK method.

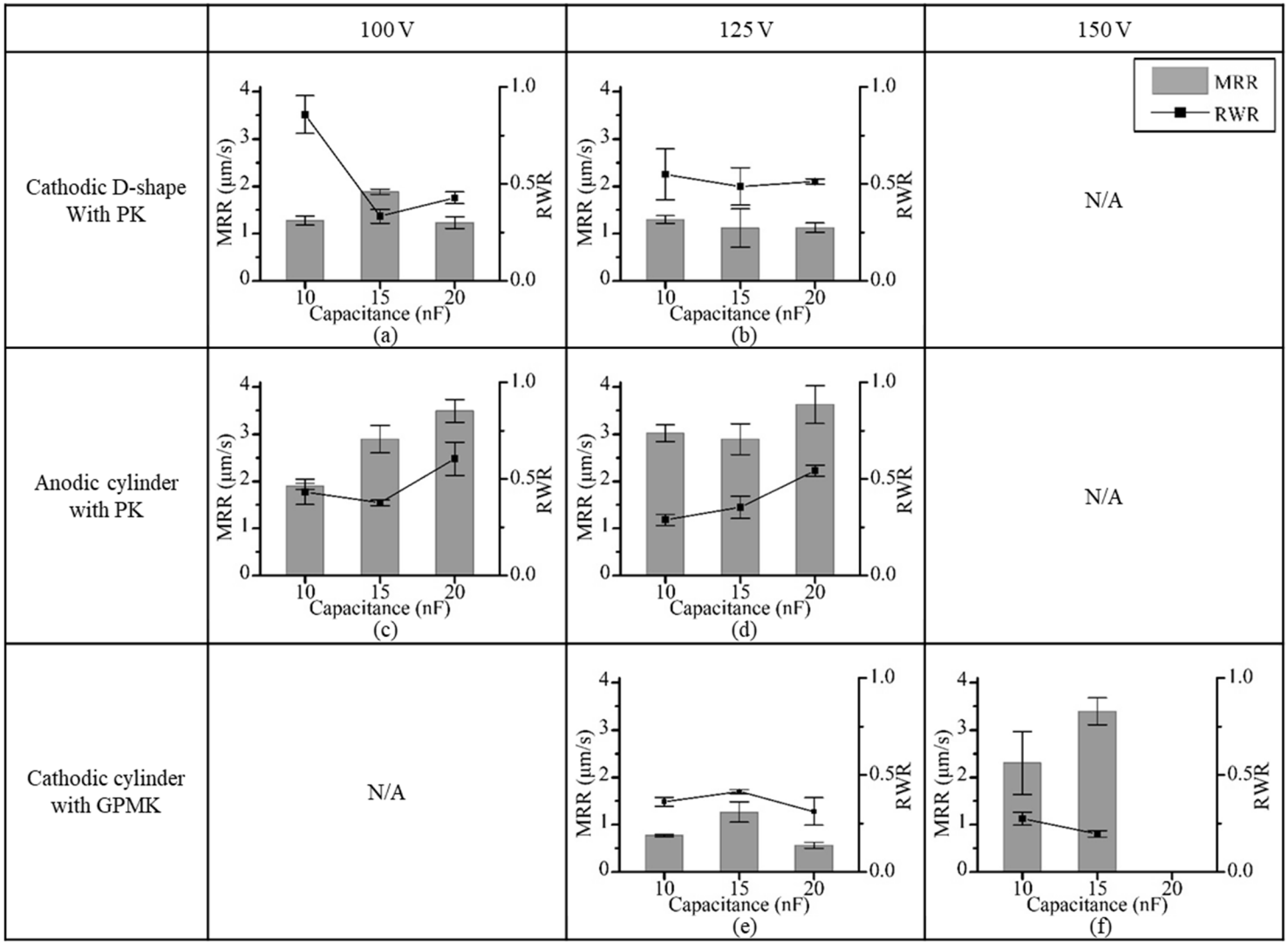

Figure 3.6 Machining results: (a) (b) cathodic D-shape with pure kerosene (PK), (c) (d) anodic cylinder with PK, and (e) (f) cathodic cylinder with graphite-powder-mixed kerosene (GPMK)

Using the anodic cylinder with PK, the open voltage of 150 V could not machine the AlN due to excessive explosion pressure. Given that the negatively charged CL on the machined surface consisted of aluminum and carbon, the machining procedures were stable and the MRRs were higher than for the cathodic D-shape with PK. Moreover, this method showed a lower RWR than the cathodic D-shape with PK method because the tool's surface area was doubled. Under several machining conditions, 125 V with 10 nF showed the lowest RWR, with a relatively high MRR.

The cathodic cylinder with GPMK behaved differently than the methods described above. As explained in section 3.3.1, the peak current for the GPMK was lower than for the PK. Thus, with an open voltage of 100 V, the tool could not reach a depth of 300 μm. In contrast, with an open voltage of 150 V and 20 nF, the excessive explosion pressure of the dielectric fluid disconnected the CL from the AE. As indicated by comparing Figures 3.6(e) and 3.6(f), 150 V resulted in a higher MRR due to sufficient discharge energy. Moreover, the RWRs were slightly decreased because of the lower number of short and hold cases in the tool feed control. As a result, 150 V with 15 nF was chosen for the cathodic cylinder with GPMK.

3.5 Performance evaluation of micro ED-drilling

Using the optimal conditions for each machining method, thru-holes with an inlet diameter of 140 μm were machined into an AlN specimen. Since GPMK has a larger discharge gap than PK, the tool diameter for the GPMK was adjusted to 50 μm, while the tool diameter for the PK was 120 μm. Figure 3.7 shows the SEM images of the inlets and outlets of the holes machined using each method. Figure 3.8 shows the MRR and RWR for each machining condition. The cathodic cylinder with GPMK showed the highest MRR and the lowest RWR of all three conditions. In addition to the GPMK's characteristics of high MRR and low RWR, sufficient supply of kerosene through the enlarged discharge gap contributed to the machining performance.

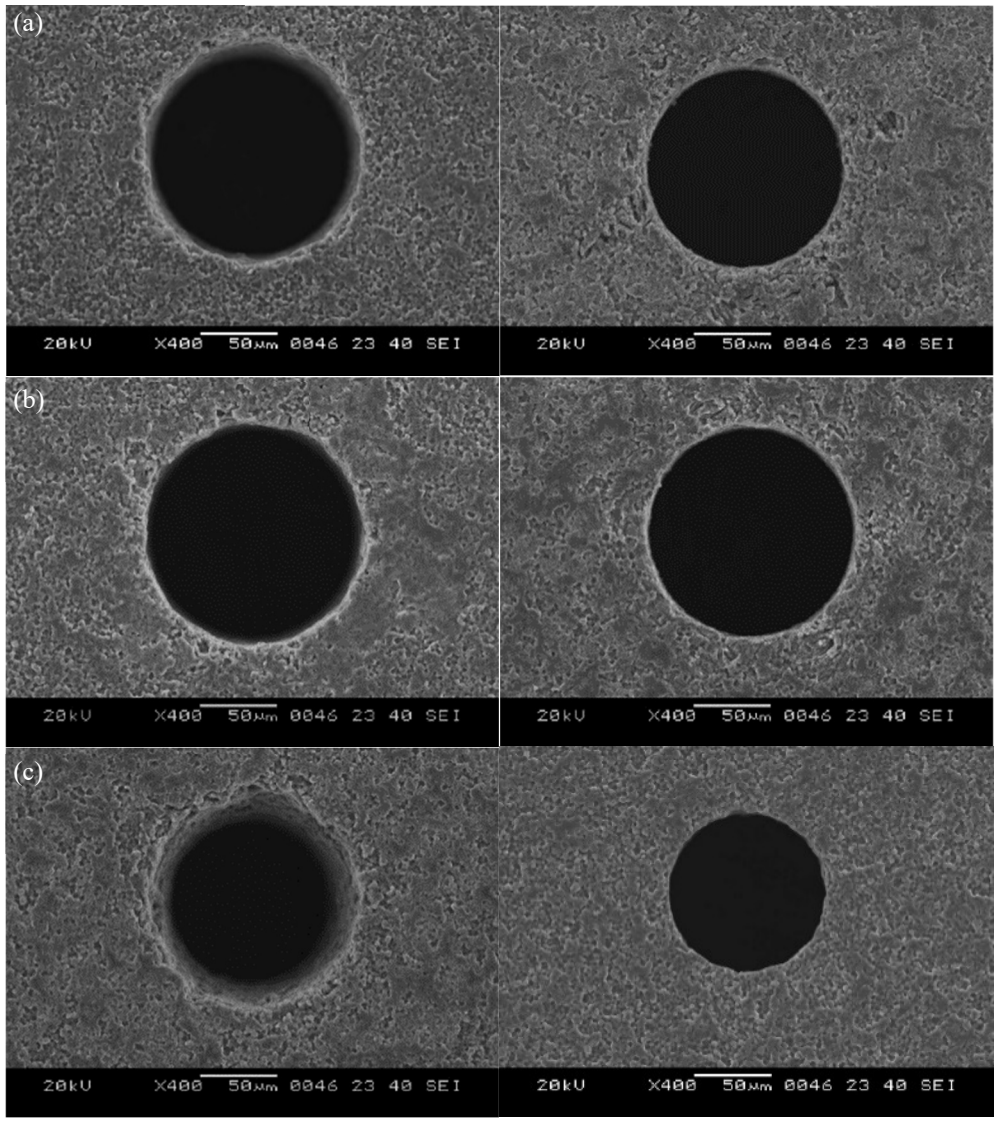

Figure 3.7 Hole inlets and outlets using (a) cathodic D-shape with pure kerosene (PK), (b) anodic cylinder with PK, and (c) cathodic cylinder with graphite-powder-mixed kerosene (GPMK)

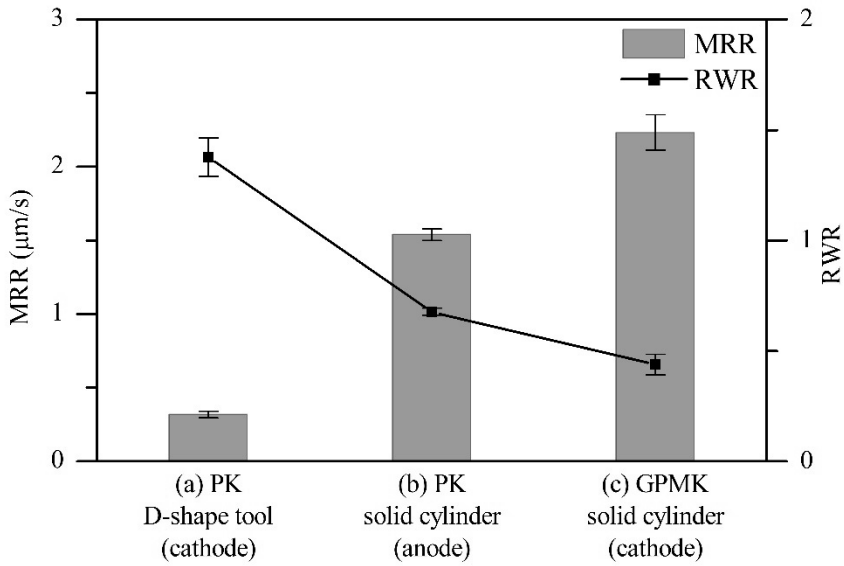

Figure 3.8 Thru-hole machining results for (a) cathodic D-shape with pure kerosene (PK), (b) anodic cylinder with PK, and (c) cathodic cylinder with graphite-powder-mixed kerosene (GPMK)

3.6 Variable voltage method for GPMK

For the GPMK thru-hole, the sizes of the inlet and outlet of the machined hole were very different (Figure 3.7), indicating a large taper angle. As shown in the cross section of the GPMK thru-hole (Figure 3.9), the inlet of the machined hole was severely tapered. In the GPMK case, because the open voltage was 150 V and the AE had low resistance, the peak current and the discharge energy were excessive. Due to the high brittleness of AlN, the explosion pressure of the kerosene created by the excessive discharge energy generated cracks and a severe taper shape at the inlet of the machined hole. After machining the AE layer, discharge with the CL occurred, which generated lower discharge energy than the AE layer due to the higher resistance of the CL.

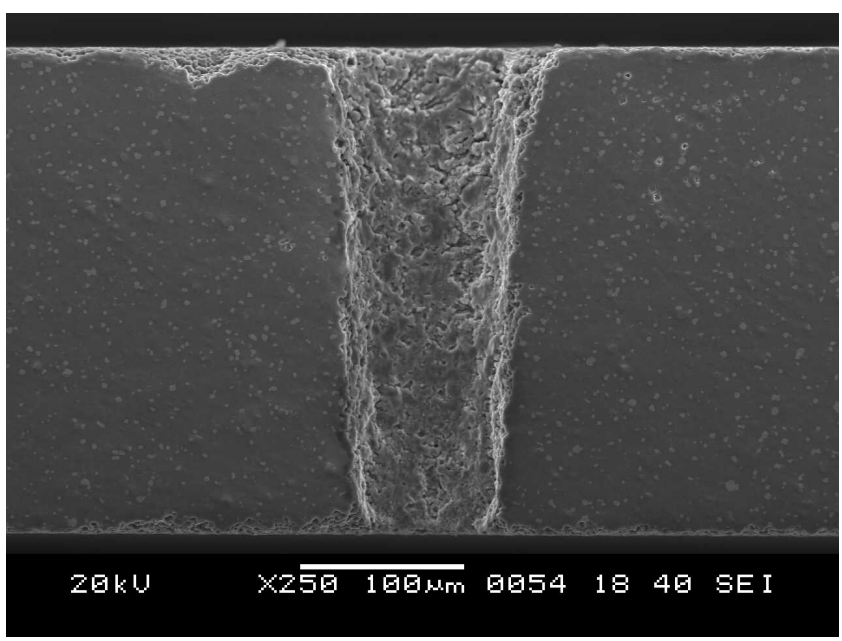

Figure 3.9 Cross section of hole machined by the constant voltage method

To solve the severe taper shapes, thru-hole machining was performed using the variable voltage method, which linearly increased the voltage as machining proceeded, as shown in Figure 3.10. Hole inlet and outlet using the variable voltage method are shown in Figure 3.11. Moreover, Figure 3.12 compares the taper angles between the four methods. The taper angle decreased by up to 0.961º. Figure 3.13 shows the GPMK thru-hole cross section machined using the variable voltage method.

Figure 3.14 compares the MRR and RWR of the GPMK with both the constant voltage and variable voltage methods. As the machining proceeded using the variable voltage, it was possible to alleviate the severe taper shape by supplying the appropriate discharge energy at the start of the machining process. As shown in Figure 3.14, using the variable voltage method increased the MRR and decreased the RWR. The variable voltage method resulted in 13% more MRR and 60% less RWR compared with the constant voltage method. For the constant voltage method, a 50 μm diameter tool was used to fit the hole inlet due to the severe taper shape. For the variable voltage method, a 70 μm diameter tool was used to fit the hole inlet. Hence, the reduction in RWR was achieved because of the increased surface area of the tool.

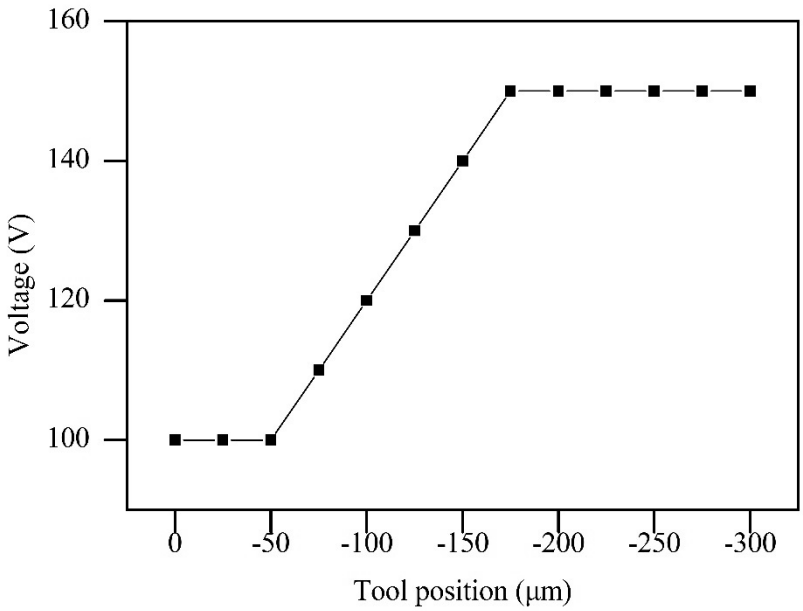

Figure 3.10 Variable voltage method

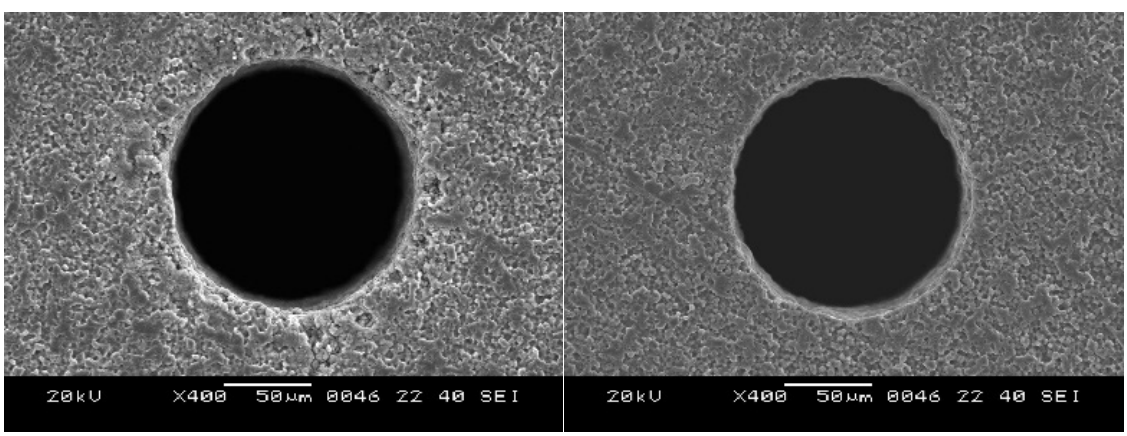

Figure 3.11 Hole inlet and outlet machined by the variable voltage method

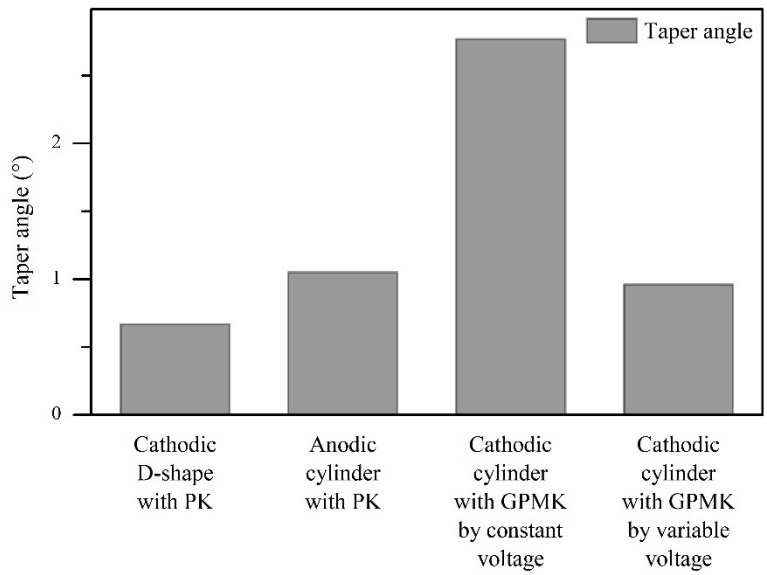

Figure 3.12 Taper angle results

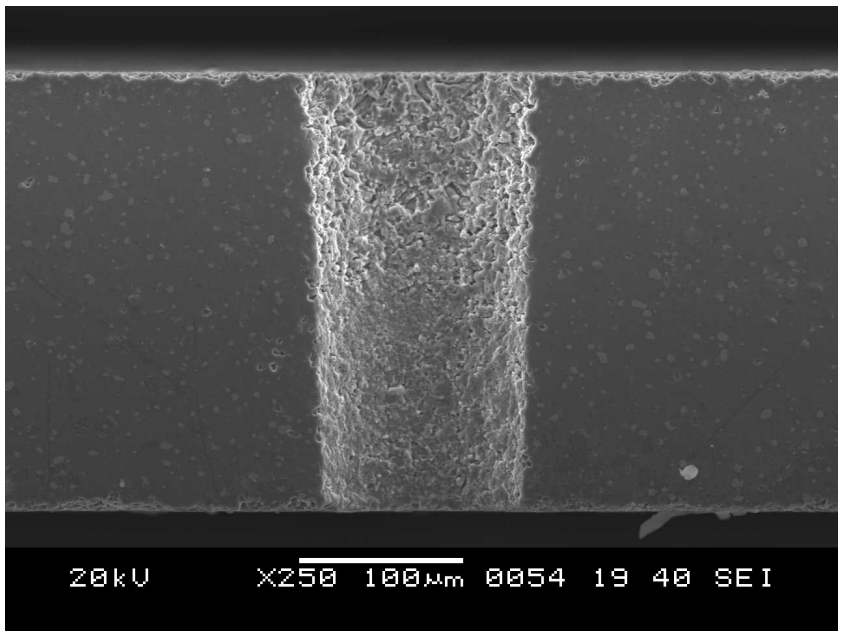

Figure 3.13 Cross section of hole machined by the variable voltage method

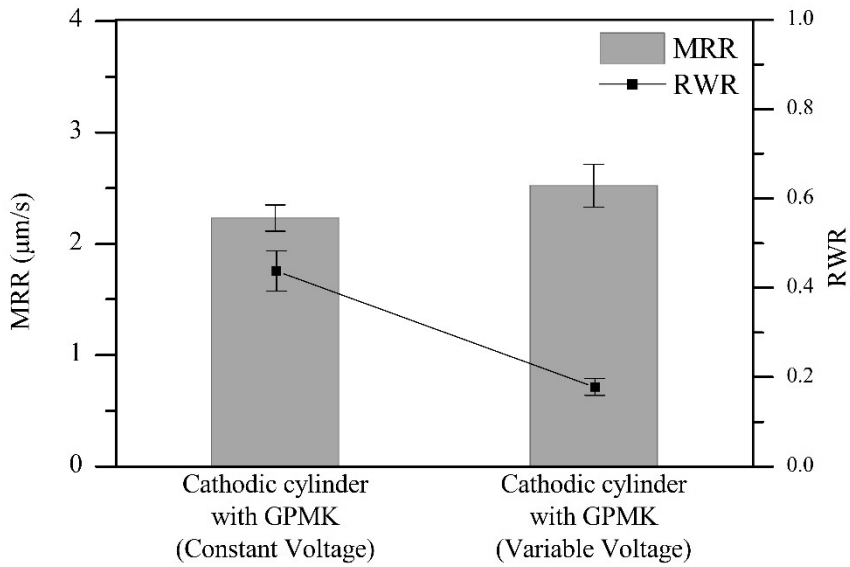

Figure 3.14 Thru-hole machining results of the constant and variable voltage methods

Chapter 4

Conclusion

This study proposed a new explanation for the effects of kerosene supply on AlN EDM and presented two methods that facilitate the ready flow of kerosene. It was found that the generation of a CL, influenced by the supply of kerosene, allows for the EDM of non-conductive AlN. We compared experimental and simulated results regarding the relationship of peak current with CL resistance. We then simulated the three methods (Cylinder tool with PK, D-shape tool with PK and cylinder tool with GPMK) to analyze the effect of each method on kerosene supply. The D-shape tool with PK and the cylinder tool with GPMK allowed the kerosene to readily flow onto the machined surface.

To find the optimal conditions for AlN micro ED-drilling, this study compared the MRRs and RWRs of the three methods. Micro thru-hole machining with identical hole diameters was then performed with different diameter tools to examine the discharge gap. These experiments indicated that facilitated kerosene flow increases the performance of AlN ED drilling. In the case of GPMK, the variable voltage method was used to resolve the tapered shape. The results showed that the cathodic cylinder with GPMK using the variable voltage method increased the MRR by 64% and decreased the RWR by 73% compared with the anodic cylinder with PK.

References

[1] Samant AN, Dahotre NB. Laser machining of structural ceramics-A review. J Eur Ceram Soc 2009;29:969–93.

[2] Taylor KM, Lenie C. Some Properties of Aluminum Nitride. J Electrochem Soc 2007;107:308.

[3] Boey FYC, Song XL, Gu ZY, Tok A. AlON phase formation in a tape-cast Al2O3/AlN composite. J Mater Process Technol 1999;89–90:478–80.

[4] Yan BH, Huang FY, Chow HM. Study on the turning characteristics of alumina-based ceramics. J Mater Process Tech 1995;54:341–7.

[5] Allor RL, Jahanmir S. Current problems and future directions for ceramic machining. Am Ceram Soc Bull 1996;75.

[6] Scheller W. Conventional Machining of Green Aluminum/ Aluminum Nitride Ceramics. Ohio J Sci 1994;94:151–4.

[7] Li JZ, Wu T, Yu ZY, Zhang L, Chen GQ, Guo DM. Micro machining of pre-sintered ceramic green body. J Mater Process Technol 2012;212:571–9.

[8] Gilbert T, Krstic VD, Zak G. Machining of aluminium nitride with ultra-violet and near-infrared Nd:YAG lasers. J Mater Process Technol 2007;189:409–17.

[9] Lumpp JK. Excimer laser machining and metallization of vias in aluminium nitride. Mater Sci Eng B 1997;45:208–12.

[10] Katahira K, Ohmori H, Uehara Y, Azuma M. ELID grinding characteristics and surface modifying effects of aluminum nitride (AlN) ceramics. Int J Mach Tools Manuf 2005;45:891–6.

[11] Kaneko K, Fukuzawa Y. Characteristics of Micro EDM for Insulating Aluminum Nitride Ceramics. Adv Mater Res 2012;579:86–91.

[12] Mohri N, Fukuzawa Y, Tani T, Saito N, Furutani K. Assisting Electrode Method for Machining Insulating Ceramics. CIRP Ann-Manuf Technol 1996;45:201-4

[13] Pham DT, Ivanov A, Bigot S, Popov K, Dimov S. An investigation of tube and rod electrode wear in micro EDM drilling. Int J Adv Manuf Technol 2007; 33:103–9

[14] Kaneko K, Yamashita K, Fukuzawa Y. Machining Characteristics of Insulating AlN Ceramics by Micro EDM. J Japan Soc Precis Eng 2013;79:540–6.

[15] ZAHIRUDDIN M, KUNIEDA M. Energy Distribution Ratio into Micro EDM Electrodes. J Adv Mech Des Syst Manuf 2010;4:1095–106.

[16] Kim YS, Chu CN. The Effects of Graphite Powder on Tool Wear in Micro Electrical Discharge Machining. Procedia CIRP 2018;68:553–8.

[17] Masuzawa T, Fujino M, Kobayashi K, Suzuki T, Kinoshita N. Wire Electro-Discharge Grinding for Micro-Machining. CIRP Ann-Manuf Technol 1985;34:431–4.

[18] Mohri N, Fukusima Y, Fukuzawa Y, Tani T, Saito N. Layer generation process on work-piece in electrical discharge machining. CIRP Ann-Manuf Technol 2003;52:157–60.

[19] Wong YS, Rahman M, Lim HS, Han H, Ravi N. Investigation of micro-EDM material removal characteristics using single RC-pulse discharges. J Mater Process Technol 2003;140:303–7.

국문 초록

본 논문에서는 기존 질화 알루미늄 미세 방전가공에서 문제가 되었던 공구 마모와 가공면으로의 등유 공급을 극복하기 위한 공정을 제시하였다. 일반적으로 실린더형 공구를 사용한 보조전극법이 사용되나 마이크로 스케일에서는 가공면에 등유의 공급이 어렵기에, 다양한 복합 가공 연구가 시도되고 있다. 그 중에서 D-형 공구와 흑연 파우더 혼합 등유를 통해 가공면으로의 등유 공급을 촉진시켜, 탄소로 이루어진 전도층의 생성을 원활하게 함을 전도층 모니터링과 실험적으로 증명하였다. 이를 기반으로 질화 알루미늄에 관통 구멍을 가공했으며 기존 방식보다 64%의 Material removal rate (MRR) 증가와 73%의 relative wear ratio (RWR) 감소를 얻어냈다. 더욱이 전도층 모니터링을 통해 다른 종류의 비전도성 세라믹 미세 방전가공의 활용성을 제시하였다.

주요어: 질화 알루미늄; 마이크로 방전 가공; 보조전극법; 흑연 파우더 혼합 등유

학번: 2018-20023